WARWICK
THE UNIVERSITY OF WARWICK

Original citation:
Reddy, G. N. Manjunatha, Malon, Michal, Marsh, Andrew, Nishiyama, Yusuke and Brown, Steven P.. (2016) A fast magic-angle spinning three-dimensional NMR experiment for simultaneously probing H-H and N-H proximities in solids. Analytical Chemistry, 88 (23). pp. 11412-11419.
Permanent WRAP URL:
http://wrap.warwick.ac.uk/83305

Copyright and reuse:
The Warwick Research Archive Portal (WRAP) makes this work of researchers of the University of Warwick available open access under the following conditions. Copyright © and all moral rights to the version of the paper presented here belong to the individual author(s) and/or other copyright owners. To the extent reasonable and practicable the material made available in WRAP has been checked for eligibility before being made available.

Copies of full items can be used for personal research or study, educational, or not-for-profit purposes without prior permission or charge. Provided that the authors, title and full bibliographic details are credited, a hyperlink and/or URL is given for the original metadata page and the content is not changed in any way.

Publisher's statement:
ACS AuthorChoice - This is an open access article published under an ACS AuthorChoice License, which permits copying and redistribution of the article or any adaptations for non-commercial purposes.

The version presented here may differ from the published version or, version of record, if you wish to cite this item you are advised to consult the publisher's version. Please see the 'permanent WRAP URL' above for details on accessing the published version and note that access may require a subscription.

For more information, please contact the WRAP Team at: wrap@warwick.ac.uk

warwick.ac.uk/lib-publications

This is an open access article published under a Creative Commons Attribution (CC-BY) License, which permits unrestricted use, distribution and reproduction in any medium, provided the author and source are cited.

analytical chemistry

Article

pubs.acs.org/ac

Fast Magic-Angle Spinning Three-Dimensional NMR Experiment for Simultaneously Probing H—H and N—H Proximities in Solids

G. N. Manjunatha Reddy,[†] Michal Malon,[‡,§] Andrew Marsh,[∥] Yusuke Nishiyama,[‡,§] and Steven P. Brown*[,†]

[†]Department of Physics and [∥]Department of Chemistry, University of Warwick, Coventry, CV4 7AL, United Kingdom

[‡]JEOL RESONANCE Inc., Musashino, Akishima, Tokyo 196-8558, Japan

[§]RIKEN CLST-JEOL Collaboration Centre, Yokohama, Kanagawa 230-0045, Japan

Supporting Information

ABSTRACT: A fast magic-angle spinning (MAS, 70 kHz) solid-state NMR experiment is presented that combines ^{1}H Double-Quantum (DQ) and ^{14}N—^{1}H HMQC (Heteronuclear Multiple-Quantum Coherence) pulse-sequence elements, so as to simultaneously probe H—H and N—H proximities in molecular solids. The proposed experiment can be employed in both two-dimensional (2D) and three-dimensional (3D) versions: first, a 2D ^{14}N HMQC-filtered ^{1}H-DQ experiment provides specific DQ-SQ correlation peaks for proton pairs that are in close proximities to the nitrogen sites, thereby achieving spectral filtration. Second, a proton-detected three-dimensional (3D) ^{1}H(DQ)-^{14}N(SQ)-^{1}H(SQ) experiment correlates ^{1}H(DQ)-^{1}H(SQ) chemical shifts with ^{14}N shifts such that longer range N···H—H correlations are observed between protons and nitrogen atoms with internuclear NH distances exceeding 3 Å. Both 2D and 3D versions of the proposed experiment are demonstrated for an amino acid hydrochloride salt, L-histidine·HCl·H_2O, and a DNA nucleoside, guanosine·$2H_2O$. In the latter case, the achieved spectral filtration ensures that DQ cross peaks are only observed for guanine NH and CH8 ^{1}H resonances and not ribose and water ^{1}H resonances, thus providing insight into the changes in the solid-state structure of this hydrate that occur over time; significant changes are observed in the NH and NH_2 ^{1}H chemical shifts as compared to the freshly recrystallized sample previously studied by Reddy et al., *Cryst. Growth Des.* **2015**, *15*, 5945.

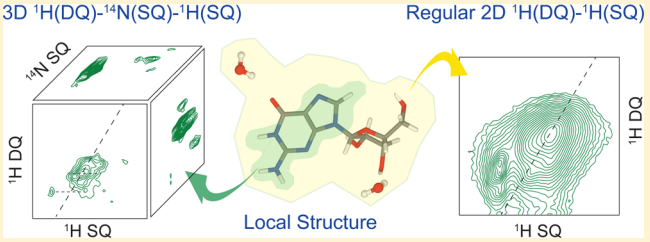

INTRODUCTION

Within the context of small and moderately sized organic molecules, ^{1}H solid-state NMR is finding increasing application for the solid-state characterization of a range of samples including pharmaceuticals, supramolecular assemblies and polymers,[1] primarily benefiting from its inherently high sensitivity even at submilligram quantities, for example, using fast magic-angle spinning (MAS) approaches.[2,3] Notably, the ^{1}H chemical shift is sensitive to intermolecular interactions such as hydrogen bonding and aromatic $\pi-\pi$ interactions, which govern molecular packing in the solid-state.[4−12] Moreover, ^{1}H detection is becoming increasingly important in biological solid-state NMR.[13−17]

Solid-state ^{1}H MAS NMR spectra of organic molecules often exhibit markedly overlapped resonances; nevertheless, 2D homonuclear ^{1}H Double-Quantum[18] (for example recorded using BaBa[19−21] recoupling), NOESY-like spin diffusion,[22,23] and heteronuclear ^{1}H—^{13}C and ^{15}N/^{14}N—^{1}H correlation experiments significantly aid spectral interpretation. Specifically, N—H proximities can be probed using a ^{14}N—^{1}H HMQC experiment[3,24−27] (^{14}N spin 1, 99.6% natural isotopic abundance) capitalizing on J couplings, dipolar couplings, and also recently on overtone ^{14}N transitions.[28−30] The ^{14}N—^{1}H HMQC experiment has been employed to characterize intermolecular N—H···N, N—H···O and O—H···N hydrogen bonding interactions in pharmaceutical cocrystals[31,32] and in the self-assembled structures adopted by modified DNA/RNA nucleosides.[33−36]

Here, a three-dimensional ^{1}H(DQ)-^{14}N(SQ)-^{1}H(SQ) correlation experiment (Figure 1) is presented whereby, under fast MAS (70 kHz), ^{1}H DQ-SQ and ^{1}H—^{14}N HMQC pulse sequence elements are concatenated. This experiment sequentially utilizes both H—H and N—H dipolar interactions for probing N···H—H proximities, and has the following advantages: first, incorporation of a ^{14}N-HMQC filter in the ^{1}H DQ experiment achieves spectral filtration by retaining only specific DQ correlation peaks for protons which are in a close proximity to nitrogen sites. This can be achieved simply by recording a 2D version of the experiment. It is to be noted that a similar approach has been proposed by Spiess and co-workers for achieving spectral simplification via ^{15}N-edited ^{1}H-DQ MAS NMR spectroscopy in keto and enol tautomers of ^{15}N-labeled

Received: May 13, 2016
Accepted: October 31, 2016
Published: October 31, 2016

 © 2016 American Chemical Society

DOI: 10.1021/acs.analchem.6b01869
Anal. Chem. 2016, 88, 11412−11419

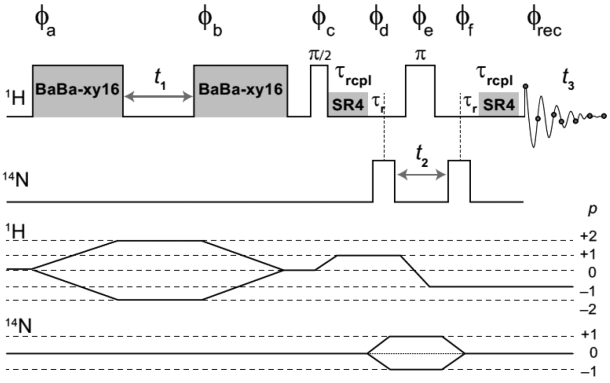

Figure 1. Pulse sequence for a three-dimensional ^{1}H(DQ)-^{14}N-(SQ)-^{1}H(SQ) correlation experiment that combines ^{1}H(DQ) spectroscopy using BaBa-xy16 recoupling and ^{14}N—^{1}H HMQC spectroscopy using SR4 recoupling pulse sequence elements. Both the ^{1}H-DQ evolution during t_1 and the ^{14}N evolution period during t_2 are rotor-synchronized with respect to the sample spinning. In the case of a 2D ^{1}H—^{14}N HMQC-filtered ^{1}H DQ-SQ correlation experiment, only the t_1 period is incremented and t_2 is set equal to one rotor period.

N-butylaminocarbonyl-6-tridecyl isocytosine.[37] Second, in a three-dimensional ^{1}H(DQ)-^{14}N(SQ)-^{1}H(SQ) experiment, proton pairs that are remotely dipolar coupled with ^{14}N sites (in which the interatomic distance between ^{14}N-sites and one of the protons in the H—H pair exceeds 3 Å) are observed. Both 2D and 3D versions of the ^{1}H(DQ)-^{14}N(SQ)-^{1}H(SQ) correlation experiment are demonstrated here for probing H—H and N—H proximities in an amino acid hydrochloride salt, L-histidine·HCl·H_2O and a dihydrate of the nucleoside guanosine, G·$2H_2O$. Our aim here is, thus, to show the applicability of the MAS NMR experiments to such small and moderately sized organic molecules.

EXPERIMENTAL AND COMPUTATIONAL DETAILS

L-histidine·HCl·H_2O and G·$2H_2O$ were purchased from Sigma-Aldrich, Gillingham, U.K. Guanosine was recrystallized from water according to the procedure described in ref 35 and stored under standard laboratory conditions.

Powder X-ray Diffraction (PXRD). Data were collected at room temperature on a Bruker D8 Advance ($K\alpha_1$ λ = 1.5406 Å) equipped with monochromatic Cu $K_{\alpha 1}$ radiation and a Ni-filtered VÅNTEC1 detector (L-Histidine·HCl·H_2O), and PANalytical X'Pert Pro MPD ($K\alpha_1$ λ = 1.5406 Å) equipped with monochromatic Cu $K_{\alpha 1}$ radiation and a PIXcel detector (G·$2H_2O$). It was verified that the samples corresponded to the HISTCM01[38] and GUANSH10[39] crystal structures—see Figures S3 and S4 in the Supporting Information (SI).

Thermogravimetric Analysis (TGA). TGA analysis was performed using a TA Q5000 instrument. Approximately 6 mg of sample was placed in an aluminum sample holder and heated over the temperature range 25−200 °C at a constant heating rate of 10 °C per minute. Helium gas was employed as a purge gas at a flow rate of 50 mL per minute.

Solid-State MAS NMR. All ^{1}H solid-state NMR experiments were performed on either a JEOL ECA700II (for L-histidine.HCl.H_2O) or a JEOL ECZ600R (for G·$2H_2O$) solid-state NMR spectrometer, equipped with a 1.0 mm double-resonance ultrafast MAS probe head (JEOL RESONANCE Inc., Tokyo, Japan). ∼0.8 mg of L-histidine·HCl·H_2O and G·$2H_2O$ were packed individually into JEOL 1 mm rotors. The ^{1}H and ^{14}N pulse lengths were experimentally optimized using a one-dimensional version of the pulse sequence shown in Figure 1. The ^{1}H $\pi/2$ pulse duration was 0.92 μs in the HMQC pulse sequence element, while a ^{1}H (nominal) $\pi/2$ pulse duration of 0.5 μs (with the same rf nutation frequency) was used in the BaBa-xy16 block. The ^{14}N pulse duration was 10 μs.

^{1}H One-Pulse. Sixteen transients were coadded using a recycle delay of 6 s (L-histidine·HCl·H_2O) or 3 s (G·$2H_2O$).

^{13}C CPMAS. 1D ^{13}C CPMAS experiments were performed on a Bruker Avance III 500 MHz (^{13}C, 125 MHz) spectrometer equipped with a 4.0 mm triple resonance MAS probe (operating in double resonance mode). For the sample stored 1 year after recrystallization, 42 mg of G.$2H_2O$ was packed into a 4 mm (outer diameter) rotor. ^{1}H and ^{13}C $\pi/2$ pulse lengths were 2.5 and 3.5 μs, respectively. The cross-polarization contact time was 1.5 ms. Heteronuclear decoupling using SPINAL64[40] with a ^{1}H pulse duration of 5 μs was applied for an acquisition time of 30 ms. 2048 transients were coadded using a relaxation delay of 3 s for a total experimental time of 2 h.

^{1}H Double-Quantum (DQ) Spectroscopy. Eight rotor periods (corresponding to 114 μs) of BaBa-xy16 recoupling was used for the excitation and reconversion of DQ coherences—the BaBa-xy16 sequence consists of a train of 32 $\pi/2$ pulses synchronized to eight rotor periods.[21] A 16-step phase cycle was used in order to select a change in coherence order $\Delta p = \pm 2$ on the DQ excitation pulses (4 steps) and $\Delta p = -1$ (4 steps) on the *z*-filter 90° pulse, where *p* is the coherence order. For both L-histidine·HCl·H_2O and G·$2H_2O$, 32 t_1 FIDs, each with 16 coadded transients, were acquired using the States-TPPI method to achieve sign discrimination in the F_1 dimension with a rotor-synchronized t_1 increment of 14.3 μs. The total experimental times was 1.7 h using a 6 s recycle delay for L-histidine·HCl·H_2O and 45 min for G.$2H_2O$ using a 3 s relaxation delay.

^{14}N(SQ)-^{1}H(SQ) HMQC. SR4 recoupling[41] was used to reintroduce the heteronuclear ^{14}N−^{1}H dipolar couplings. On the first ^{1}H $\pi/2$ pulse, a 4-step nested phase cycle [2(0), 2(180), 2(90), 2(270)] was applied to select Δp = +1, while a 2-step [0, 180] phase cycle was applied on the last ^{14}N pulse in order to select $\Delta p = \pm 1$, with the receiver phase [0, 2(180), 0, 270, 2(90), 270]. For each of 16 t_1 FIDs (using the States-TPPI method to achieve sign discrimination in F_1 with a rotor synchronized increment of 14.3 μs), for L-histidine·HCl·H_2O, 4 transients were coadded with a recycle delay of 6 s corresponding to a total experimental time of 12 min, while for G·$2H_2O$, 48 transients were coadded with a recycle delay of 3 s corresponding to a total experimental time of 2 h 35 min.

^{1}H(DQ)-^{14}N(SQ) HMQC-^{1}H(SQ). A BaBa-xy16 sequence[21] is used for the excitation of DQ coherence and reconversion of DQ into SQ coherence, with the resulting DQ-filtered SQ coherence being the starting point for a subsequent ^{14}N—^{1}H HMQC pulse sequence element. The BaBa-xy16 part is phase cycled to observe DQ coherences and the HMQC part is phase cycled to select the SQ coherence pathways. In the HMQC part, the SR4 pulse sequence was applied during the excitation and reconversion periods to decouple the ^{1}H homonuclear dipolar interactions and recouple the ^{1}H—^{14}N heteronuclear dipolar interactions.[41] For the pulse sequence shown in Figure 1, the phase cycling is given as follows: (a) [2(0), 2(90), 2(180), 2(270)]; (b) [8(0), 8(90), 8(180), 8(270)]; (c) [0]; (d) [(0, 180), (0, 180)]; (e) [32(0), 32(120), 32(240)]; (f) [0] and (rec) [2(0, 180, 180, 0), 2(180, 0, 0, 180), 2(0, 180, 180, 0), 2(180, 0, 0, 180), 2(240, 60, 60, 240), 2(60, 240, 240, 60), 2(240, 60, 60, 240), 2(60, 240, 240, 60), 2(120, 300, 300, 120),

DOI: 10.1021/acs.analchem.6b01869
Anal. Chem. 2016, 88, 11412−11419

2(300, 120, 120, 300), 2(120, 300, 300, 120), and 2(300, 120, 120, 300)]. Both the t_1 duration for ^{1}H DQ evolution and the t_2 duration for ^{14}N evolution are rotor synchronized with the sample spinning, i.e., $t_1 = m\tau_r$ and $t_2 = n\tau_r$, where m and n are integers.

In the case of the 2D version of the ^{1}H(DQ)-^{14}N(SQ)-^{1}H-(SQ) experiment, only the t_1 period was incremented. A total of 24 t_1 FIDs were acquired using the States-TPPI method to achieve sign discrimination in F_1 with a rotor synchronized increment of 14.3 μs. For L-histidine·HCl·H_2O, 96 transients were coadded with a recycle delay of 6 s corresponding to a total experimental time of 7.7 h, while for G·2H_2O, 32 transients were coadded with a recycle delay of 3 s corresponding to a total experimental time of about 5.5 h.

In the case of 3D experiments, an array of 16 t_1 × 16 t_2 FIDs were collected in the ^{1}H DQ and ^{14}N SQ dimensions using the States-TPPI method. For L-histidine·HCl·H_2O, 32 transients were coadded with a recycle delay of 5 s corresponding to a total experimental time of 45.5 h., while for G·2H_2O, 96 transients were coadded with a recycle delay of 3 s corresponding to a total experimental time of 82 h.

All ^{1}H chemical shifts are calibrated with respect to neat TMS using adamantane (1.85 ppm) as an external reference.[42] ^{14}N chemical shifts were referenced to neat CH_3NO_2 using powdered NH_4Cl at −341.2 as an external reference (see Table 2 of ref 43). To convert to the chemical shift scale frequency used in protein NMR, where the alternative IUPAC (see Appendix 1 of ref 44) reference is liquid NH_3 at −50 °C, it is necessary to add 379.5 ppm to the given values.[45]

GIPAW DFT Calculations. All calculations were performed using plane-wave based DFT implemented within the Cambridge Serial Total Energy Package (CASTEP) code, U.K. academic release version 8.0.[46] Atomic coordinates were obtained from the crystal structure of L-histidine.HCl.H_2O, as previously solved by X-ray diffraction: CSID code HISTCM01, $Z = 4$, $Z' = 1$, space group $P2_1$, 100 atoms/unit cell (including 1 HCl and 1 H_2O).[38] In a first stage, a geometry optimization is performed: starting with the crystal structure, the positions of all atoms are allowed to move (with the unit cell parameters fixed, and space group symmetry imposed as determined from the X-ray diffraction structure) until an energy-minimized structure is obtained. The distances stated in this paper correspond to this geometry-optimized crystal structure. NMR shielding calculations were performed using the Gauge-Including Projector-Augmented Wave (GIPAW) approach.[47,48]

Both geometry optimization and NMR chemical shift calculations used a plane-wave basis set and the PBE exchange correlation functional[48,49] at a basis cutoff energy of 600 eV with integrals taken over the Brillouin zone by using a Monkhorst−Pack grid of minimum sample spacing 0.08 × 2π Å^{-1}. A semiempirical dispersion correction was applied using the TS scheme[50] for both geometry optimization and NMR shielding calculations with on-the-fly (OTF) ultrasoft pseudopotentials.[51] Forces, stress on the unit cell, energy and displacements were converged to better than 0.01 eV Å^{-1}, 0.1 G Pa, 0.000 000 4 eV, and 0.001 Å, respectively.

RESULTS AND DISCUSSION

L-Histidine·HCl·H_2O. A single-pulse ^{1}H (700 MHz, 70 kHz MAS) spectrum is presented in Figure 2a: the higher ppm peaks assigned to H5 and H7 correspond to protons exhibiting intermolecular N—H···O hydrogen bonding interactions. Figure 2 presents ^{1}H DQ-SQ correlation spectra recorded

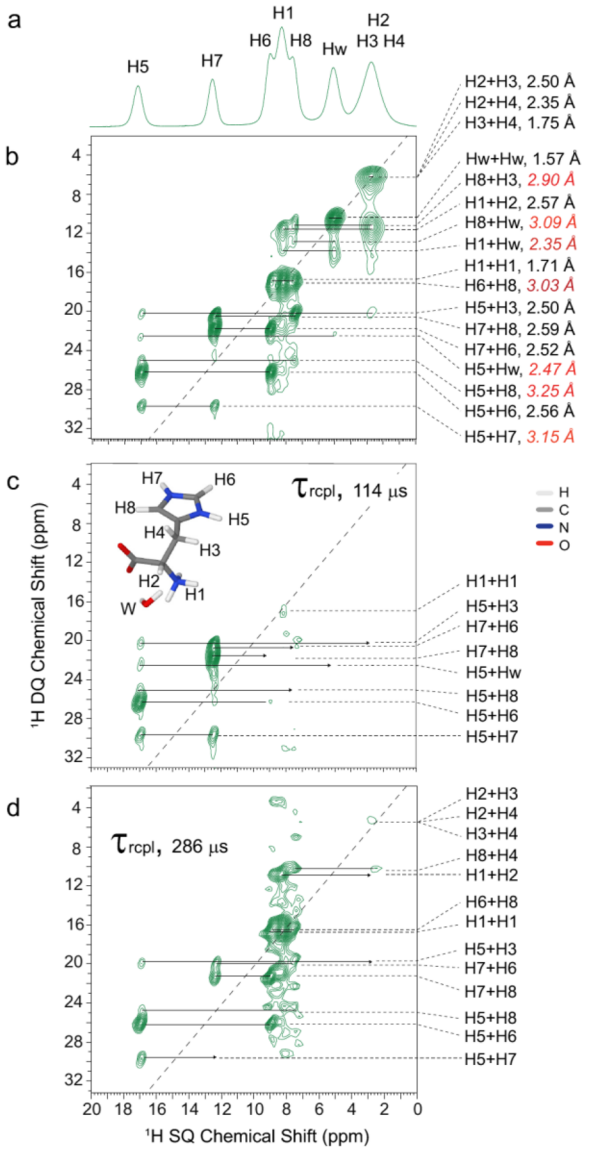

Figure 2. Experimental ^{1}H NMR spectra recorded at 700 MHz using 70 kHz MAS are presented for L-histidine·HCl·H_2O: (a) a ^{1}H single-pulse spectrum, (b) a ^{1}H DQ-SQ correlation spectrum (recorded using 8 τ_r of BaBa-xy16 recoupling[21]), (c, d) ^{14}N-HMQC filtered ^{1}H DQ-SQ spectra recorded using (c) a short (τ_{rcpl} = 114 μs) and (d) a long (τ_{rcpl} = 286 μs) recoupling duration. In (b), interatomic H—H distances are presented together with the ^{1}H DQ peak assignments (values in red italics are intermolecular H—H proximities). The base contour levels are at (b) 14%, (c) 25%, and (d) 30% of the maximum peak intensity.

without (Figure 2b) and with a ^{14}N-HMQC filter (Figure 2c,d): the DQ peaks in Figure 2b are labeled by the corresponding H—H proximities (within 3.3 Å, as obtained from the DFT geometry optimized structure of L-histidine·HCl·H_2O). ^{1}H SQ and DQ chemical shifts together with the H—H proximities are listed in Table S1, while GIPAW DFT calculated ^{1}H chemical shielding values are given in Table S2. Rows extracted from the regular 2D ^{1}H DQ and the ^{14}N-HMQC filtered ^{1}H DQ spectra are presented for the DQ peaks at 5.8, 10.3, 16.0, and 29.4 ppm in Figure S1.

In a ^{14}N-HMQC filtered ^{1}H DQ-SQ spectrum recorded using a short recoupling time (114 μs, Figure 2c), DQ-SQ peaks are only retained for proton pairs where one or both

DOI: 10.1021/acs.analchem.6b01869
Anal. Chem. 2016, 88, 11412−11419

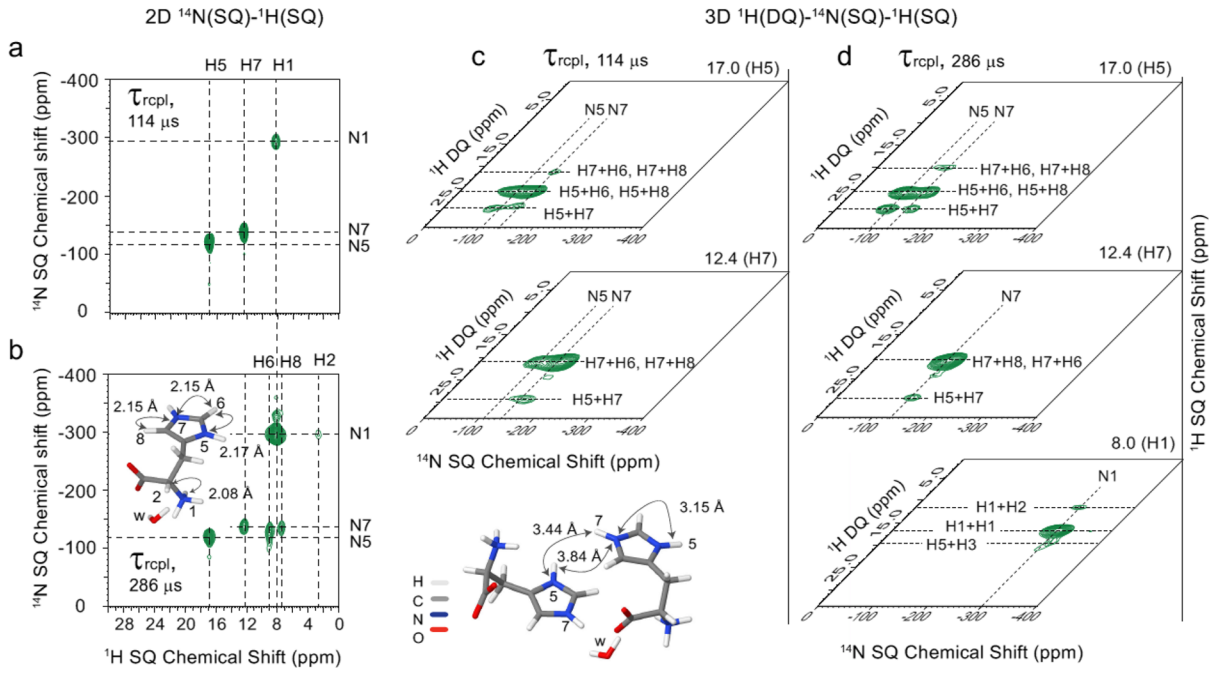

Figure 3. (a, b) 2D ^{14}N(SQ)-^{1}H(SQ) spectra and (c, d) 2D ^{14}N(SQ)-^{1}H(DQ) planes extracted from 3D ^{1}H(DQ)-^{14}N(SQ)-^{1}H(SQ) spectra of L-histidine·HCl·H_2O. Data were acquired at a ^{1}H Larmor frequency of 700 MHz and an MAS frequency of 70 kHz using n = 2 rotary resonance recoupling for a τ_{rcpl} duration of (a and c) 114 μs and (b and d) 286 μs. The base contour levels are at (a) 25%, (b) 31%, (c) 36%, and (d) 43% of the maximum peak intensity.

Table 1. N—H Proximities in L-Histidine·HCl·H_2O Corresponding to the N—H Correlations Observed in Figure 3c,d

L-histidine·HCl·H_2O	
chemical site	N···H distance (Å)
N1···H2	2.08
N5···H6	2.17
N5···H7	3.19, 3.44[a]
N7···H5	3.15, 3.84[a]
N7···H6	2.15
N7···H8	2.15

[a]intermolecular H−H proximities.

protons are directly bonded to a ^{14}N site, i.e., for the ring NH (H5 and H7) and NH_3 (H1) protons. Note that low intensity for the NH_3 (H1) peak is attributed to the rotation of the NH_3 protons reducing the magnitude of the ^{14}N—^{1}H dipolar coupling by which magnetization transfer is achieved. In the ^{14}N-filtered DQ spectrum recorded by using a longer recoupling duration (286 μs, Figure 2d), ^{1}H DQ-SQ peaks are recovered for the NH_3 (H1) peak and the imidazole ring protons (H6 and H8) for which the nearest N···H distances are between 2.15 and 2.17 Å. It is evident from Figure 2c,d that the spectral complexity in the ^{1}H DQ spectra can be readily tuned by varying the recoupling duration, thus aiding spectral interpretation.

The left-hand side of Figure 3 presents ^{14}N(SQ)-^{1}H(SQ) spectra recorded with the same recoupling durations as for the ^{14}N-HMQC filtered ^{1}H DQ-SQ spectra presented in Figure 2c,d, namely a short 114 μs (Figure 3a) and a longer 286 μs (Figure 3b) recoupling duration. As was the case for the spectra in Figure 2, by changing the recoupling duration, the spectroscopist can select the number of correlation peaks that

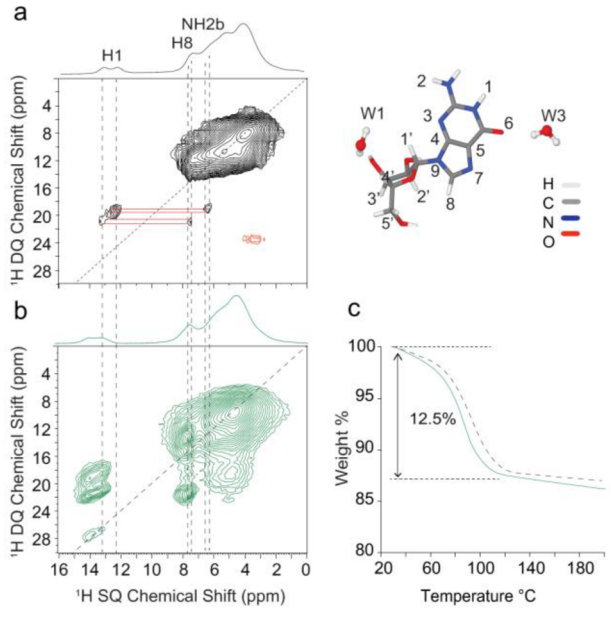

Figure 4. (a, b) Comparison of ^{1}H one-pulse and two-dimensional DQ MAS NMR spectra of guanosine samples: (a) recorded directly after recrystallization from water (^{1}H 850 MHz, 75 kHz MAS, DQ MAS spectrum recorded using 1 τ_r of BaBa recoupling, 13.3 μs, reproduced from Figures 3 and S2 of ref 35) and (b) a DQ MAS spectrum recorded after storage under standard laboratory conditions a year later at 600 MHz using 70 kHz MAS and 8 τ_r of BaBa-xy16 recoupling, 114 μs. (c) Thermogravimetric analysis of the guanosine sample—note that a 12.5% weight loss corresponds to a dihydrate form, G·2H_2O. Black dashed line and green solid lines correspond to TGA analysis carried out directly after the recrystallization from water (reproduced from Figure 2 of ref 35) and after a year being stored under laboratory conditions, respectively.

DOI: 10.1021/acs.analchem.6b01869
Anal. Chem. 2016, 88, 11412−11419

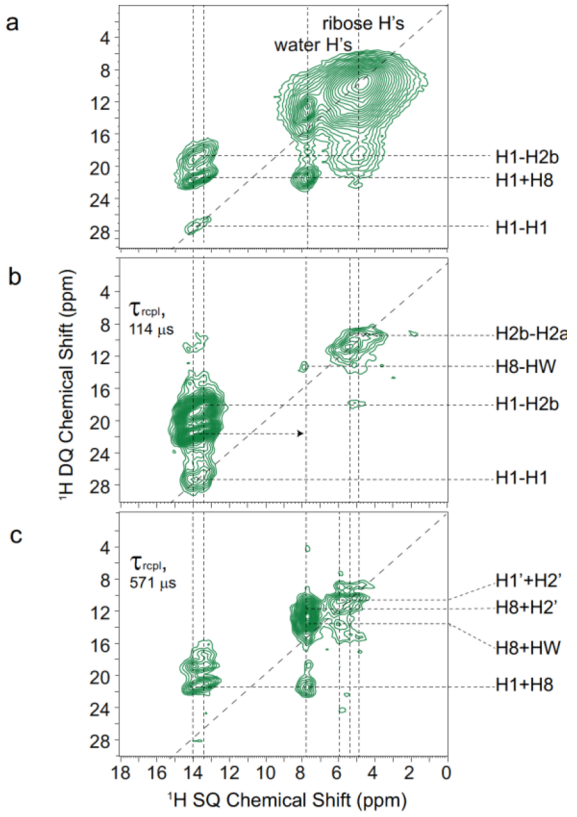

Figure 5. Experimental ^{1}H NMR spectra recorded at 600 MHz using 70 kHz MAS are presented for G.2H_2O: (a−c) ^{1}H DQ-SQ correlation spectra (recorded using 8 τ_r of BaBa-xy16 recoupling), (a) repeated from Figure 4b, for (b and c) a ^{14}N—^{1}H HMQC filter was employed using a (b) short (τ_{rcpl} = 114 μs = 6 τ_r) and a (c) long (τ_{rcpl} = 571 μs = 20 τ_r) recoupling time. The base contour levels are at (a) 4%, (b) 13%, and (c) 22% of the maximum peak intensity.

are observed. Specifically, only one-bond N7—H7, N5—H5, and N1—H1 correlations are observed in Figure 3a, whereas longer range correlations are observed in Figure 3b for N5—H6, N7—H6, and N7—H8, corresponding to internuclear N—H distances of 2.17, 2.15, and 2.15 Å, respectively. Thus, there is an evident analogy to the observation of ^{1}H DQ peaks for the H6 and H8 resonances in Figure 2d (for the longer recoupling duration). Note that Table S3 lists calculated (GIPAW) ^{14}N chemical shieldings and quadrupolar parameters for L-histidine·HCl·H_2O and compares the calculated and experimental ^{14}N shifts.

Figure 3 also presents spectral planes extracted from two different ^{1}H(DQ)-^{14}N(SQ)-^{1}H(SQ) HMQC three-dimensional experimental data sets. Such a 3D experiment (see Figure 1) permits the sampling, in the first and second indirect dimensions (i.e., t_1 and t_2), of both ^{1}H DQ and ^{14}N(SQ) coherences, while benefiting from the advantage of ^{1}H detection[52−55](i.e., during the acquisition period, t_3). From the cuboid resulting from a three-dimensional Fourier transformation, it is possible to extract planes corresponding to two of the three spectral dimensions at a fixed frequency in the third dimension. As shown in Figure 3c and 3d, it is of most interest to consider ^{14}N(SQ)-^{1}H(DQ) planes extracted at the ^{1}H SQ chemical shifts corresponding to the three directly bonded NH moieties for which cross peaks are observed in Figure 3a, i.e., at 17.0 ppm (H1, NH), 12.4 ppm (H7, NH) and 8.0 ppm (H1, NH_3). The planes presented in Figure 3c and 3d correspond to two different 3D experiments using the two distinct recoupling times of 114 and 286 μs, respectively.

The most intense peaks in the planes shown in Figure 3c,d are at the H5 + H6 ^{1}H DQ frequency for the H5 ^{1}H SQ frequency (top); the H7 + H6 and H7 + H8 ^{1}H DQ frequency (H6 and H8 ^{1}H chemical shifts are too close to resolve in this experiment) for the H7 ^{1}H SQ frequency (middle); and the H1 + H1 ^{1}H DQ frequency for the H1 ^{1}H SQ frequency (bottom). Thus, these correspond to a correlation between a nitrogen SQ coherence and a DQ coherence involving the directly bonded hydrogen, i.e., (top) N5···H5, (middle) N7···H7 and (bottom) N1···H1, and a nearby second proton, i.e., (top) H5—H6 (2.56 Å), (middle) H7—H6 (2.52 Å), and H7—H8 (2.59 Å) and (bottom) H1—H1 (1.71 Å).

It is also important to observe that the ^{14}N(SQ)-^{1}H(DQ) planes at the H5 (17 ppm) ^{1}H chemical shift display a N5···H5—H7 correlation peak and likewise the ^{14}N(SQ)-^{1}H(DQ) planes at the H7 chemical shift (12.4 ppm) display a N7···H5—H7 correlation peak. Note that the closest H—H proximity for this H5—H7 DQ coherence is an intermolecular proximity of 3.19 Å, with the intramolecular proximity being 4.12 Å. In such a case, the contribution of multiple different H—H distances is reflected in a root-sum squared dipolar coupling, with the intensity of a ^{1}H DQ peak depending, to a first approximation, on the square of this root-sum squared dipolar coupling,[56,57] i.e., the contribution of the closer intermolecular proximity compared to the intramolecular proximity to the H5—H7 DQ can be estimated as $4.12^6/3.19^6 \sim 5$. As listed in Table 1 and illustrated by the inset in the bottom left of Figure 3, the corresponding N5···H7 and N7···H5 distances are 3.44 and 3.84 Å (intermolecular) and 3.19 and 3.15 Å (intramolecular), which is significantly longer than the under 2.2 Å longer-range nitrogen hydrogen distances for the cross peaks observed in the 2D ^{14}N(SQ)-^{1}H(SQ) spectrum in Figure 3b.

Guanosine·2H_2O. Supramolecular assemblies generated from guanosine (G) derivatives have a wide range of applications such as lyotropic mesophases, gelators, thin-films, and synthetic ion channels.[58,59] The formation of ribbon-like assemblies in the absence of cations, mainly driven by intermolecular N—H···N and N—H···O hydrogen bonding interactions, is well-known.[34,35,39,60,61] A crystal structure of guanosine, G·2H_2O, has been solved by X-ray diffraction; there is a ribbon-like assembly whereby two crystallographically independent molecules, namely A and B, self-organize in the form of -A-A-A-A- and -B-B-B-B-.[39] In this structure, there are two types of water molecules: interlayer water (W1 and W2 interconnect the sugar moieties of adjacent G-ribbons) and intralayer water (W3 and W4 interconnecting the two-dimensional sheets of guanine frames) that reinforce the three-dimensional stacking of ribbons by means of intermolecular O−H···O hydrogen bonds (Figure S4).[35,39,62,63]

Figure 4a reproduces from ref 35 (Figures 3 and S2) a 1D ^{1}H and 2D ^{1}H DQ-SQ MAS spectrum of G·2H_2O as recorded directly after the recrystallization from water. As shown in Figure S4, it was verified by PXRD that this sample corresponds to the published crystal structure, GUANSH10.[39] For this recrystallized sample, after storage for a year under laboratory conditions, 1D ^{1}H and 2D ^{1}H DQ-SQ MAS spectra were recorded again as shown in Figure 4b. There is an evident change in the spectra, with this being consistent with the PXRD pattern (see Figure S4) having also changed considerably. Notably, the ^{1}H chemical shifts of the NH1 and NH_2 protons

DOI: 10.1021/acs.analchem.6b01869
Anal. Chem. 2016, 88, 11412−11419

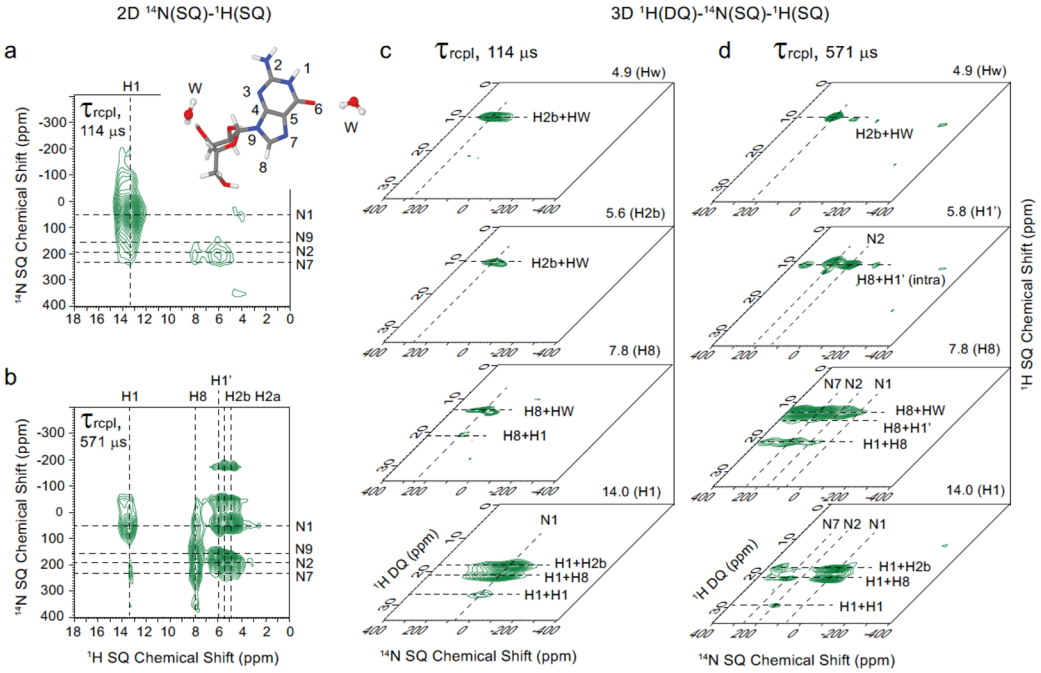

Figure 6. (a, b) 2D ^{14}N(SQ)-^{1}H(SQ) spectra and (c, d) 2D ^{14}N(SQ)-^{1}H(DQ) planes extracted from 3D ^{1}H(DQ)-^{14}N(SQ)-^{1}H(SQ) spectra are presented for G·2H$_2$O. Spectra were recorded at a ^{1}H Larmor frequency of 600 MHz and an MAS frequency of 70 kHz using n = 2 rotary resonance recoupling for a τ_{rcpl} duration of (a and c) 114 μs and (b and d) 571 μs. The base contour levels are at (a) 29%, (b) 36%, (c) 31%, and (d) 42% of the maximum peak intensity.

have changed and in Figure 4b, DQ auto peaks are observed for the NH1 protons at δ_{DQ} = 13.2 + 13.2 = 26.4 and 13.8 + 13.8 = 27.6 ppm, with no such peaks being observed in Figure 4a.

Sugawara and co-workers have observed changes in PXRD patterns for the solid-state structures of guanosine associated with changing moisture content; using molecular dynamics (MD), they have identified that the intralayer water molecules (W3 and W4) have a relatively weak affinity to the G-ribbons, hence offering an explanation for the humidity-induced changes in solid-state structure.[62,63] Figure 4c compares thermogravimetric analysis (TGA) of G·2H$_2$O, carried out directly after the recrystallization from water (black dashed lines, also presented in Figure 2 of ref 35) and performed a year later after the sample had been stored at laboratory conditions (green solid line). Both samples showed 12.5% weight loss corresponding to the dihydrate form of guanosine, but minor changes are observed in the TGA curves in the temperature range 40 °C to 120 °C, suggesting variations in affinity of water molecules within the crystal lattice that are in line with the experimental observations and MD simulations of Sugawara and co-workers.[62,63] We show here the structural insight that can be gained from the new solid-state NMR experiment described above for the case of this guanosine dihydrate sample (stored under laboratory conditions for a year after recrystallization) for which there is no crystal structure available. In addition, a comparison of ^{13}C cross-polarization (CP) MAS spectra of an as-received guanosine sample, the fresh recrystallized sample and the sample in this work is given in Figure S4; the corresponding ^{13}C chemical shifts are stated in Table S4, noting that Sugawara et al. have presented ^{13}C CPMAS spectra reported in Figure 3 of ref 62.

2D ^{14}N-HMQC filtered ^{1}H DQ-SQ correlation spectra recorded by using a short (114 μs) and a long (571 μs) recoupling time are presented in Figure 5b,c, respectively; for comparison, a standard ^{1}H DQ spectrum presented in Figure 5a is repeated from Figure 4b above. Specific rows extracted from the 2D ^{14}N-HMQC filtered ^{1}H DQ-SQ correlation spectra are presented in Figure S5. The advantage of the spectral filtration achieved in this case for the crowded spectral region for δ_{SQ} between 3 and 9 ppm is evident. Specific DQ cross peaks become visible that are otherwise obscured by the broad ribose and water ^{1}H SQ resonances.

In order to assign the observed ^{1}H DQ peaks in Figure 5, consider first the complementary insight that is provided by the two-dimensional ^{14}N—^{1}H spectra in Figure 6a,b that were recorded with the same short (114 μs) and a long (571 μs) recoupling time. In Figure 6a, cross peaks corresponding to the one-bond N—H connectivities in the NH (NH1) and NH$_2$ (NH2a and NH2b) moieties are observed, while in Figure 6b, cross peaks corresponding to longer range N···H proximities involving the H8 and sugar protons (H1′) and the non-protonated nitrogen resonances (N7, N9) appear. Returning to Figure 5, it can then be identified that in Figure 5b (τ_{rcpl} = 114 μs), DQ-SQ peaks are largely only observed for the NH (H1) and NH$_2$ (NH2a and NH2b) ^{1}H SQ resonances, while for the spectrum in Figure 5c (τ_{rcpl} = 571 μs), DQ peaks are additionally seen for the CH8 ^{1}H SQ resonance that has a close (<2.2 Å) intramolecular NH proximity. Importantly, this allows the assignment of ^{1}H DQ cross peaks at 4.9 + 13.3 = 18.2 ppm between NH (H1) and the NH2b protons in Figure 5b and at 13.3 + 7.8 = 21.1 ppm between NH (H1) and the H8 protons in Figure 5c. As shown for other guanosine derivatives, the changes in SQ and DQ frequencies for such peaks can be structurally informative about different modes of self-assembly.[33−35,64]

As was the case with L-histidine·HCl·H$_2$O above, further insight is provided by considering Figure 6c,d which present ^{1}H(DQ)-^{14}N(SQ) planes extracted from 3D ^{1}H(DQ)-^{14}N-(SQ)-^{1}H(SQ) data sets at ^{1}H SQ chemical shifts of 4.9, 5.6, 7.8, and 14.0 ppm corresponding to the water (Hw), NH2b, H8

DOI: 10.1021/acs.analchem.6b01869
Anal. Chem. 2016, 88, 11412−11419

and NH (H1) protons, respectively. The planes in Figure 6c correspond to a short (114 μs) duration of recoupling of the ^{14}N—^{1}H dipolar interaction such that, as in Figure 6a, strongest intensity is observed at the N1 ^{14}N shift for the plane at the NH (H1) ^{1}H SQ chemical shift. In this case, intense peaks are observed at the H1 + H8 and H1 + H2b ^{1}H DQ chemical shifts as in Figure 5b, corresponding to N1···H8 and N1···H2b longer-range proximities. For the planes in Figure 6d corresponding to a long (571 μs) recoupling duration, peaks are also observed at the other nitrogen resonances: consider the plane at the H8 ^{1}H SQ chemical shift, strong intensity is observed for ^{1}H DQ peaks involving the H8 proton and the N7 and also the N1 nitrogen. Such information about specific longer-range nitrogen hydrogen distances could be useful for testing structural models for this guanosine dihydrate structure, e.g., those deriving from a MD simulation such as in ref 63.

CONCLUSIONS

This study presents 2D and 3D versions of a ^{1}H(DQ)-^{14}N-(SQ)-^{1}H(SQ) NMR experiment for probing simultaneously H—H proximities and N—H proximities under fast MAS conditions. Experimental results are demonstrated for an amino acid salt, L-histidine·HCl·H_2O and a DNA base, G·2H_2O. 2D ^{14}N-edited ^{1}H DQ-SQ spectra retain specific DQ peaks for proton-pairs that are dipolar coupled with ^{14}N sites. This type of spectral filtration led to the observation of specific DQ peaks involving the H8 and NH2 protons in G·2H_2O, which are otherwise lost under DQ peaks due to ribose and water protons in a standard ^{1}H DQ-SQ correlation spectrum. Furthermore, a 3D ^{1}H(DQ)-^{14}N(SQ)-^{1}H(SQ) correlation experiment allows the observing of long-range ^{14}N—^{1}H correlations, as shown for N···H distances exceeding 3 Å for L-histidine·HCl·H_2O.

The ^{1}H(DQ)-^{14}N(SQ)-^{1}H(SQ) experiment is complementary to previously reported ^{15}N-filtered ^{1}H DQ-SQ[37] (^{15}N isotopic labeling was required) experiments as well as ^{1}H DQ-^{13}C SQ or ^{14}N-filtered ^{1}H—^{13}C correlation experiments (larger sample quantities are required).[65−67] The proposed experiment is particularly useful for obtaining specific structural information or monitoring temporal changes in the vicinity of NH sites. This approach could be further extended to probe H—H proximities in the vicinity of other NMR active quadrupolar nuclei, e.g., chlorine[68] which will also benefit from the use of higher magnetic field strength under fast MAS conditions.

ASSOCIATED CONTENT

Supporting Information

The Supporting Information is available free of charge on the ACS Publications website at DOI: 10.1021/acs.analchem.6b01869.

Table of experimental DQ chemical shifts for L-histidine·HCl·H_2O, table of GIPAW calculated ^{1}H NMR shieldings and ^{14}N quadrupolar parameters for L-histidine·HCl·H_2O together with comparison to experiment, rows extracted from 2D ^{1}H DQ spectra for L-histidine·HCl·H_2O and G·2H_2O, comparison of experimental PXRD patterns with simulated PXRD patterns for L-histidine·HCl·H_2O and G·2H_2O, ^{13}C CP MAS spectra of the different G.2H_2O samples. The experimental and calculated data for this study are provided as a supporting data set from WRAP, the Warwick Research Archive Portal at http://wrap.warwick.ac.uk/http://wrap.warwick.ac.uk/83295 (PDF)

AUTHOR INFORMATION

Corresponding Author

*E-mail: S.P.Brown@warwick.ac.uk.

Notes

The authors declare no competing financial interest.

ACKNOWLEDGMENTS

We acknowledge funding from EPSRC (EP/K003674/1). We thank Dr. Manoj Pandey for assistance with solid-state NMR experiments. GIPAW DFT calculations were performed on the University of Warwick Centre for Scientific Computing (CSC) cluster. Dr. Ben Douglas, Department of Chemistry is thanked for help with thermogravimetric analysis and Dr. David Walker (University of Warwick) is thanked for PXRD measurements. The PXRD, DSC-TGA and some computing facilities used in this research were obtained through Birmingham Science City: Innovative Uses for Advanced Materials in the Modern World with support from Advantage West Midlands (AWM) and part funded by the European Regional Development Fund (ERDF).

REFERENCES

(1) Brown, S. P. *Solid State Nucl. Magn. Reson.* **2012**, *41*, 1.
(2) Samoson, A.; Tuherm, T.; Gan, Z. *Solid State Nucl. Magn. Reson.* **2001**, *20*, 130.
(3) Nishiyama, Y.; Endo, Y.; Nemoto, T.; Utsumi, H.; Yamauchi, K.; Hioka, K.; Asakura, T. *J. Magn. Reson.* **2011**, *208*, 44.
(4) Yates, J. R.; Pham, T. N.; Pickard, C. J.; Mauri, F.; Amado, A. M.; Gil, A. M.; Brown, S. P. *J. Am. Chem. Soc.* **2005**, *127*, 10216.
(5) Schmidt, J.; Hoffmann, A.; Spiess, H. W.; Sebastiani, D. *J. Phys. Chem. B* **2006**, *110*, 23204.
(6) Brouwer, D. H.; Alavi, S.; Ripmeester, J. A. *Phys. Chem. Chem. Phys.* **2008**, *10*, 3857.
(7) Gowda, C. M.; Vasconcelos, F.; Schwartz, E.; van Eck, E. R. H.; Marsman, M.; Cornelissen, J.; Rowan, A. E.; de Wijs, G. A.; Kentgens, A. P. M. *Phys. Chem. Chem. Phys.* **2011**, *13*, 13082.
(8) Mafra, L.; Santos, S. M.; Siegel, R.; Alves, I.; Paz, F. A. A.; Dudenko, D.; Spiess, H. W. *J. Am. Chem. Soc.* **2012**, *134*, 71.
(9) Dudenko, D. V.; Williams, P. A.; Hughes, C. E.; Antzutkin, O. N.; Velaga, S. P.; Brown, S. P.; Harris, K. D. M. *J. Phys. Chem. C* **2013**, *117*, 12258.
(10) Xu, J.; Terskikh, V. V.; Chu, Y.; Zheng, A.; Huang, Y. *Chem. Mater.* **2015**, *27*, 3306.
(11) Fernandes, J. A.; Sardo, M.; Mafra, L.; Choquesillo-Lazarte, D.; Masciocchi, N. *Cryst. Growth Des.* **2015**, *15*, 3674.
(12) Baias, M.; Lesage, A.; Aguado, S.; Canivet, J.; Moizan-Basle, V.; Audebrand, N.; Farrusseng, D.; Emsley, L. *Angew. Chem., Int. Ed.* **2015**, *54*, 5971.
(13) Zhou, D. H.; Shea, J. J.; Nieuwkoop, A. J.; Franks, W. T.; Wylie, B. J.; Mullen, C.; Sandoz, D.; Rienstra, C. M. *Angew. Chem., Int. Ed.* **2007**, *46*, 8380.
(14) Agarwal, V.; Penzel, S.; Szekely, K.; Cadalbert, R.; Testori, E.; Oss, A.; Past, J.; Samoson, A.; Ernst, M.; Böckmann, A.; Meier, B. H. *Angew. Chem., Int. Ed.* **2014**, *53*, 12253.
(15) Knight, M. J.; Webber, A. L.; Pell, A. J.; Guerry, P.; Barbet-Massin, E.; Bertini, I.; Felli, I. C.; Gonnelli, L.; Pierattelli, R.; Emsley, L.; Lesage, A.; Herrmann, T.; Pintacuda, G. *Angew. Chem., Int. Ed.* **2011**, *50*, 11697.
(16) Lamley, J. M.; Iuga, D.; Öster, C.; Sass, H.-J.; Rogowski, M.; Oss, A.; Past, J.; Reinhold, A.; Grzesiek, S.; Samoson, A.; Lewandowski, J. R. *J. Am. Chem. Soc.* **2014**, *136*, 16800.
(17) Wang, S.; Parthasarathy, S.; Xiao, Y.; Nishiyama, Y.; Long, F.; Matsuda, I.; Endo, Y.; Nemoto, T.; Yamauchi, K.; Asakura, T.; Takeda,

DOI: 10.1021/acs.analchem.6b01869
Anal. Chem. 2016, 88, 11412−11419

M.; Terauchi, T.; Kainosho, M.; Ishii, Y. *Chem. Commun.* **2015**, *51*, 15055.
(18) Brown, S. P. *Prog. Nucl. Magn. Reson. Spectrosc.* **2007**, *50*, 199.
(19) Sommer, W.; Gottwald, J.; Demco, D. E.; Spiess, H. W. *J. Magn. Reson., Ser. A* **1995**, *113*, 131.
(20) Schnell, I.; Lupulescu, A.; Hafner, S.; Demco, D. E.; Spiess, H. W. *J. Magn. Reson.* **1998**, *133*, 61.
(21) Saalwächter, K.; Lange, F.; Matyjaszewski, K.; Huang, C.-F.; Graf, R. *J. Magn. Reson.* **2011**, *212*, 204.
(22) Elena, B.; Emsley, L. *J. Am. Chem. Soc.* **2005**, *127*, 9140.
(23) Elena, B.; Pintacuda, G.; Mifsud, N.; Emsley, L. *J. Am. Chem. Soc.* **2006**, *128*, 9555.
(24) Cavadini, S.; Antonijevic, S.; Lupulescu, A.; Bodenhausen, G. *J. Magn. Reson.* **2006**, *182*, 168.
(25) Gan, Z. H.; Amoureux, J. P.; Trebosc, J. *Chem. Phys. Lett.* **2007**, *435*, 163.
(26) Siegel, R.; Trébosc, J.; Amoureux, J.-P.; Gan, Z. *J. Magn. Reson.* **2008**, *193*, 321.
(27) Cavadini, S. *Prog. Nucl. Magn. Reson. Spectrosc.* **2010**, *56*, 46.
(28) Nishiyama, Y.; Malon, M.; Gan, Z.; Endo, Y.; Nemoto, T. *J. Magn. Reson.* **2013**, *230*, 160.
(29) O'Dell, L. A.; He, R.; Pandohee, J. *CrystEngComm* **2013**, *15*, 8657.
(30) Haies, I. M.; Jarvis, J. A.; Bentley, H.; Heinmaa, I.; Kuprov, I.; Williamson, P. T. F.; Carravetta, M. *Phys. Chem. Chem. Phys.* **2015**, *17*, 6577.
(31) Tatton, A. S.; Pham, T. N.; Vogt, F. G.; Iuga, D.; Edwards, A. J.; Brown, S. P. *CrystEngComm* **2012**, *14*, 2654.
(32) Maruyoshi, K.; Iuga, D.; Antzutkin, O. N.; Alhalaweh, A.; Velaga, S. P.; Brown, S. P. *Chem. Commun.* **2012**, *48*, 10844.
(33) Webber, A. L.; Masiero, S.; Pieraccini, S.; Burley, J. C.; Tatton, A. S.; Iuga, D.; Pham, T. N.; Spada, G. P.; Brown, S. P. *J. Am. Chem. Soc.* **2011**, *133*, 19777.
(34) Reddy, G. N. M.; Cook, D. S.; Iuga, D.; Walton, R. I.; Marsh, A.; Brown, S. P. *Solid State Nucl. Magn. Reson.* **2015**, *65*, 41.
(35) Reddy, G. N. M.; Marsh, A.; Davis, J. T.; Masiero, S.; Brown, S. P. *Cryst. Growth Des.* **2015**, *15*, 5945.
(36) Robertson, A. J.; Pandey, M. K.; Marsh, A.; Nishiyama, Y.; Brown, S. P. *J. Magn. Reson.* **2015**, *260*, 89.
(37) Schnell, I.; Langer, B.; Söntjens, S. H. M.; van Genderen, M. H. P.; Sijbesma, R. P.; Spiess, H. W. *J. Magn. Reson.* **2001**, *150*, 57.
(38) Oda, K.; Koyama, H. *Acta Crystallogr., Sect. B: Struct. Crystallogr. Cryst. Chem.* **1972**, *28*, 639.
(39) Thewalt, U.; Bugg, C. E.; Marsh, R. E. *Acta Crystallogr., Sect. B: Struct. Crystallogr. Cryst. Chem.* **1970**, *26*, 1089.
(40) Fung, B.; Khitrin, A.; Ermolaev, K. *J. Magn. Reson.* **2000**, *142*, 97.
(41) Brinkmann, A.; Kentgens, A. P. M. *J. Am. Chem. Soc.* **2006**, *128*, 14758.
(42) Hayashi, S.; Hayamizu, K. *Bull. Chem. Soc. Jpn.* **1991**, *64*, 685.
(43) Hayashi, S.; Hayamizu, K. *Bull. Chem. Soc. Jpn.* **1991**, *64*, 688.
(44) Harris, R. K.; Becker, E. D.; Cabral de Menezes, S. M.; Granger, P.; Hoffman, R. E.; Zilm, K. W. *Pure Appl. Chem.* **2008**, *80*, 59.
(45) Martin, G. E.; Hadden, C. E. *J. Nat. Prod.* **2000**, *63*, 543.
(46) Clark, S. J.; Segall, M. D.; Pickard, C. J.; Hasnip, P. J.; Probert, M. J.; Refson, K.; Payne, M. C. *Z. Kristallogr. - Cryst. Mater.* **2005**, *220*, 567.
(47) Pickard, C. J.; Mauri, F. *Phys. Rev. B: Condens. Matter Mater. Phys.* **2001**, *63*, 245101.
(48) Yates, J. R.; Pickard, C. J.; Mauri, F. *Phys. Rev. B: Condens. Matter Mater. Phys.* **2007**, *76*, 024401.
(49) Perdew, J. P.; Burke, K.; Ernzerhof, M. *Phys. Rev. Lett.* **1996**, *77*, 3865.
(50) Tkatchenko, A.; Scheffler, M. *Phys. Rev. Lett.* **2009**, *102*, 073005.
(51) Vanderbilt, D. *Phys. Rev. B: Condens. Matter Mater. Phys.* **1990**, *41*, 7892.
(52) Ishii, Y.; Tycko, R. *J. Magn. Reson.* **2000**, *142*, 199.
(53) Paulson, E. K.; Morcombe, C. R.; Gaponenko, V.; Dancheck, B.; Byrd, R. A.; Zilm, K. W. *J. Am. Chem. Soc.* **2003**, *125*, 15831.
(54) Reif, B.; Griffin, R. G. *J. Magn. Reson.* **2003**, *160*, 78.
(55) Nishiyama, Y. *Solid State Nucl. Magn. Reson.* **2016**, *78*, 24.
(56) Zorin, V. E.; Brown, S. P.; Hodgkinson, P. *Mol. Phys.* **2006**, *104*, 293.
(57) Bradley, J. P.; Tripon, C.; Filip, C.; Brown, S. P. *Phys. Chem. Chem. Phys.* **2009**, *11*, 6941.
(58) Davis, J. T. *Angew. Chem., Int. Ed.* **2004**, *43*, 668.
(59) Davis, J. T.; Spada, G. P. *Chem. Soc. Rev.* **2007**, *36*, 296.
(60) Mande, S. S.; Seshadri, T. P.; Viswamitra, M. A. *Acta Crystallogr., Sect. C: Cryst. Struct. Commun.* **1989**, *45*, 92.
(61) Giorgi, T.; Grepioni, F.; Manet, I.; Mariani, P.; Masiero, S.; Mezzina, E.; Pieraccini, S.; Saturni, L.; Spada, G. P.; Gottarelli, G. *Chem. - Eur. J.* **2002**, *8*, 2143.
(62) Sugawara, Y.; Iimura, Y.; Iwasaki, H.; Urabe, H.; Saito, H. *J. Biomol. Struct. Dyn.* **1994**, *11*, 721.
(63) Yoneda, S.; Sugawara, Y.; Urabe, H. *J. Phys. Chem. B* **2005**, *109*, 1304.
(64) Peters, G. M.; Skala, L. P.; Plank, T. N.; Oh, H.; Manjunatha Reddy, G. N.; Marsh, A.; Brown, S. P.; Raghavan, S. R.; Davis, J. T. *J. Am. Chem. Soc.* **2015**, *137*, 5819.
(65) Bradley, J. P.; Velaga, S. P.; Antzutkin, O. N.; Brown, S. P. *Cryst. Growth Des.* **2011**, *11*, 3463.
(66) Amoureux, J.-P.; Trébosc, J.; Hu, B.; Halpern-Manners, N.; Antonijevic, S. *J. Magn. Reson.* **2008**, *194*, 317.
(67) Webber, A. L.; Elena, B.; Griffin, J. M.; Yates, J. R.; Pham, T. N.; Mauri, F.; Pickard, C. J.; Gil, A. M.; Stein, R.; Lesage, A.; Emsley, L.; Brown, S. P. *Phys. Chem. Chem. Phys.* **2010**, *12*, 6970.
(68) Pandey, M. K.; Kato, H.; Ishii, Y.; Nishiyama, Y. *Phys. Chem. Chem. Phys.* **2016**, *18*, 6209.

DOI: 10.1021/acs.analchem.6b01869
Anal. Chem. 2016, 88, 11412−11419